JOURNAL OF CATALYSIS 86, 359–372 (1984)

# A Study of the Nickel–Titanium Oxide Interaction

A. J. SIMOENS, R. T. K. BAKER, D. J. DWYER, C. R. F. LUND, AND R. J. MADON

*Exxon Research & Engineering Company, Clinton Township, Route 22 East, Annandale, New Jersey 08801*

Received August 1, 1983; revised November 23, 1983

Previous studies have demonstrated that, when nickel supported on titanium oxide is reduced in hydrogen at 450°C and higher, the system exhibits SMSI properties. We have employed several complementary experimental approaches in an attempt to gain an insight into the intimate details surrounding the nickel–titanium oxide interaction. High resolution transmission electron microscopy was used to examine the changes in morphology of nickel particles following reduction at increasing temperatures. *In situ* ferromagnetic resonance studies have provided characterization of the state of the nickel as a function of reduction temperature. A geometrically designed catalyst in combination with scanning Auger surface analysis was used to probe transport phenomena involving nickel and titanium oxide during treatment in hydrogen. The combined results of these studies have enabled us to develop a model which involves the migration of titanium–oxygen moieties onto the surface of the nickel particles during reduction in hydrogen. This *decoration model* provides a mechanism whereby SMSI properties are observed.

## INTRODUCTION

Since Tauster and co-workers (*1, 2*) reported that Group VIIIA noble metals supported on certain oxides, including titanium oxide, lose $H_2$ and CO chemisorption capacity following reduction at temperatures in excess of 500°C, many studies of these systems have ensued. These investigations have revealed the existence of an interaction between the metals and the titanium oxide support which is termed a strong metal–support interaction (SMSI) and which has primarily been identified through suppressed hydrogen adsorption. Recent characterization studies of nickel/titanium oxide catalysts have highlighted the difficulties associated with attempts to determine the nickel crystallite size by hydrogen chemisorption following reduction of the catalysts between 450 and 750°C (*3, 4*).

The $CO/H_2$ synthesis reactions have been used as one probe to determine the catalytic consequences of the SMSI phenomenon. Vannice and Garten (*5*) found that nickel supported on reduced titanium oxide exhibited increased activity and distinctly different selectivity in these reactions, compared to more conventional nickel catalysts. Specifically, over nickel/titanium oxide the products contain higher percentages of larger molecular weight paraffins, reduced methane selectivity, and reduced nickel carbonyl formation. There were also indications that the nickel/titanium oxide had a greater tolerance toward carbon deposition and/or metal particle sintering.

Burch and Flambard (*6*) have challenged the notion that a metal–support interaction is responsible for high CO hydrogenation activity offering an alternative explanation which involves the adsorption of CO at the interface between reduced titanium oxide ($Ti_4O_7$) and the metal. Kugler and Garten (*7*) demonstrated that the addition of small quantities of $TiO_2$ to bulk nickel could effect activity and selectivity changes comparable to those measured when 10% Ni is supported on $TiO_2$.

A variety of techniques including ultraviolet photoelectron spectroscopy, X-ray photoelectron spectroscopy, Auger electron spectroscopy, and low energy electron diffraction were used by Kao and co-workers to examine the nature of the nickel/titanium oxide interaction (*8*). They concluded



0021-9517/84 $3.00

that the SMSI effect was caused by a charge transfer between nickel and titanium oxide and the extent to which this process occurred was dependent on the pretreatment of the titanium oxide. They also claimed that if specimens of nickel deposited on the $TiO_2$ (110) surface were heated to 300°C or higher then the metal diffused into the bulk oxide.

In the present work several experimental approaches have been employed in an attempt to gain a clearer insight into the intimate nature of the nickel–titanium oxide interaction. High resolution transmission electron microscopy has been used to examine the changes in morphology of nickel particles as a function of reduction temperature. From selected area electron diffraction examinations, it has been possible to obtain information about the changes in structure of the oxide support. Ferromagnetic resonance studies have provided characterization of the state of the nickel as a function of reduction temperature. Finally, a geometrically designed model catalyst in combination with scanning Auger surface analysis has been used to probe the existence of transport phenomena involving nickel and titanium oxide following treatment in hydrogen.

## EXPERIMENTAL METHODS

Electron transparent films of titanium oxide, 35-nm thick, were prepared according to the procedure described previously (*9*) and were mounted on stainless-steel electron microscope grids. Nickel was introduced onto these films by vacuum evaporation of spectrographically pure nickel wire from a heated tungsten filament. The amount of wire and distance of the specimen from the evaporation source were adjusted so that approximately a monolayer coverage of metal would be produced.

Specimens were subsequently reduced in a flowing 20% hydrogen/helium mixture for 1 hr at 150, 550, 700, and 800°C; at least three fresh specimens were used for each reduction treatment. After reaction the samples were carefully passivated by cooling in flowing helium and then treated in 2% oxygen/helium at room temperature before exposure to air. Unless this procedure was followed, the specimens underwent an exothermic reaction when taken out of the reactor. Examination of the specimens was performed in a Philips EM 300 transmission electron microscope which had a resolution of better than 0.25 nm. Particle size distribution measurements were obtained from over 600 particles which were taken from six different micrographs after each treatment.

The support material used in the preparation of samples for the ferromagnetic resonance investigation was obtained from the Cabot Corporation under the trade name Cab-O-Ti. The production and characterization of this material, along with the method of preparation of the 10% nickel/titanium oxide catalyst used in this study were described previously (*5*).

The ferromagnetic resonance studies reported here were performed with a Bruker ER-200D electron spin resonance spectrometer operating in the X-band. First-derivative spectra were obtained by scanning the magnetic field between 0 and 10 kOe, and using a modulation frequency of 100 kHz. The spectrometer was equipped with a cylindrical, water-cooled, high-temperature cavity. The sample temperature was varied by adjusting the temperature of a dry $H_2/N_2$ stream flowing upwards through the ESR cavity and around the microreactor containing the sample. The temperature was measured by a thermocouple placed in the reactor. Another thermocouple was positioned below the microreactor and outside the ESR cavity. Heating conditions were chosen to minimize the temperature gradient in the cavity. The quartz ESR reactors were designed so that the treatment gas was preheated during annular downflow before passing upward through the catalyst bed. The use of the reactors in the ESR cavity allowed spectra to be obtained while the sample experienced the same gas envi-

ronment that it had been reacted in (i.e., only the sample temperature was altered). Adsorption was effected by flowing hydrogen over the sample *in situ*; and desorption, by flowing argon (50 sccm) at 300–400°C for 20 min.

The experimental procedure and the type of information which can be derived from a ferromagnetic resonance investigation have been discussed previously (*10*). In particular, qualitative and quantitative data can be gathered on particle size and shape, degree of reduction, surface anisotropy, and support effects for the dispersed ferromagnetic metal. It is also possible with this technique to gain a measure of the hydrogen chemisorption capacity of ferromagnetic systems. Indeed hydrogen adsorption induces a relative magnetization decrease, $\Delta M/M$, which can be expressed by two relationships (*11*), depending on whether the metal particles are ferromagnetic:

$$\frac{\Delta M}{M} = \frac{N_H}{N_T} \cdot \frac{\alpha/2}{\mu_{Ni}} = \frac{I_T - I_H}{I_T} \qquad (1)$$

or superparamagnetic:

$$\frac{\Delta M}{M} = \frac{(N_H \cdot \mu_{Ni} - N_H\alpha/2)^2 - (N_T \cdot \mu_{Ni})^2}{(N_t \cdot \mu_{Ni})^2} \qquad (2)$$

In these equations, $N_T$ is the total number of nickel atoms, $N_H$ is the number of nickel atoms which chemisorb hydrogen, $\mu_{Ni}$ is the magnetic moment of one nickel atom (0.606 Bohr magneton), $\alpha$ corresponds to the magnetization loss induced by one hydrogen molecule (1.46 Bohr magnetons), and $I_H$ and $I_T$ are the room temperature FMR intensities with and without hydrogen chemisorption, respectively. Hydrogen chemisorption has also been observed to decrease the magnetostriction and/or surface anisotropy values of small supported nickel crystallites (*12–15*), resulting in line-width and line-shape asymmetry decreases.

The reactant gases used in this work, argon, oxygen, and propylene (Research Grade), were obtained from Matheson, and hydrogen was produced from distilled water in a Matheson generator which incorporated a palladium diffusion thimble. Gas flows typically ranging from 5 to 100 sccm, were regulated by Tylan mass flow controllers.

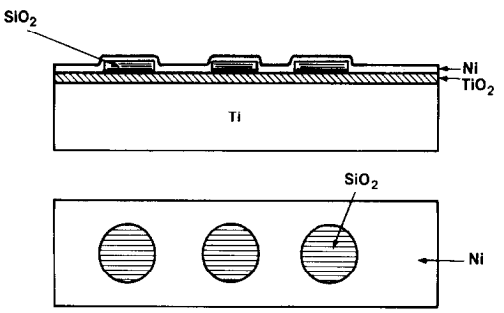


FIG. 1. Schematic representation of the geometrically designed catalyst.

In another series of experiments the concept of a geometrically designed model catalyst system was employed. This three-component system was prepared as outlined in Fig. 1. First, titanium foil (99.99% purity, 0.025-mm thick) was heated in air at 600°C for 1 h to convert the metal surface to oxide. Following the oxidation, disks of silicon dioxide (5 mm diameter and 10-nm thick) were deposited on the titanium oxide surface by vacuum evaporation of a 50/50 $Si/SiO_2$ mixture through a mask. A second air oxidation was employed to oxidize the Si. Finally, a layer of nickel, 10-nm thick was deposited over the entire surface of the specimen by vacuum evaporation.

This geometrically designed model catalyst was analyzed in a Leybold-Heraeus surface analysis system equipped with a scanning Auger microprobe and an *in situ* high pressure reactor system (*16*). Surface analysis was performed before and after reduction (450°C, 20% $H_2$/He at 1.5 atm) of the sample. Following the reduction treatment, some specimens were examined in a JEOL 35C scanning electron microscope, which had the capability of resolving 6 to 10 nm.

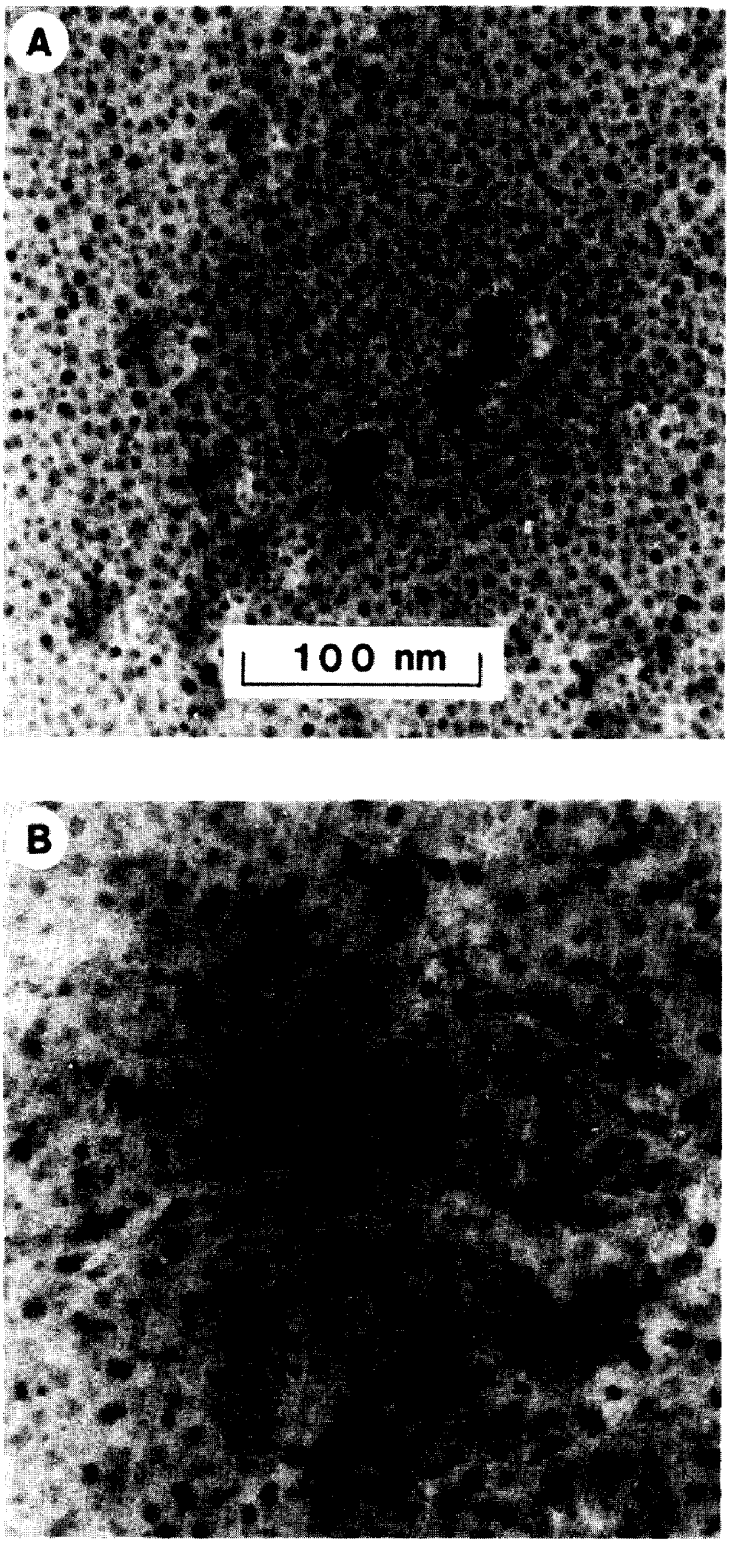


FIG. 2. The appearance of nickel on titanium oxide after reduction in hydrogen at (A) 150, (B) 550, (C) 700, and (D) 800°C.

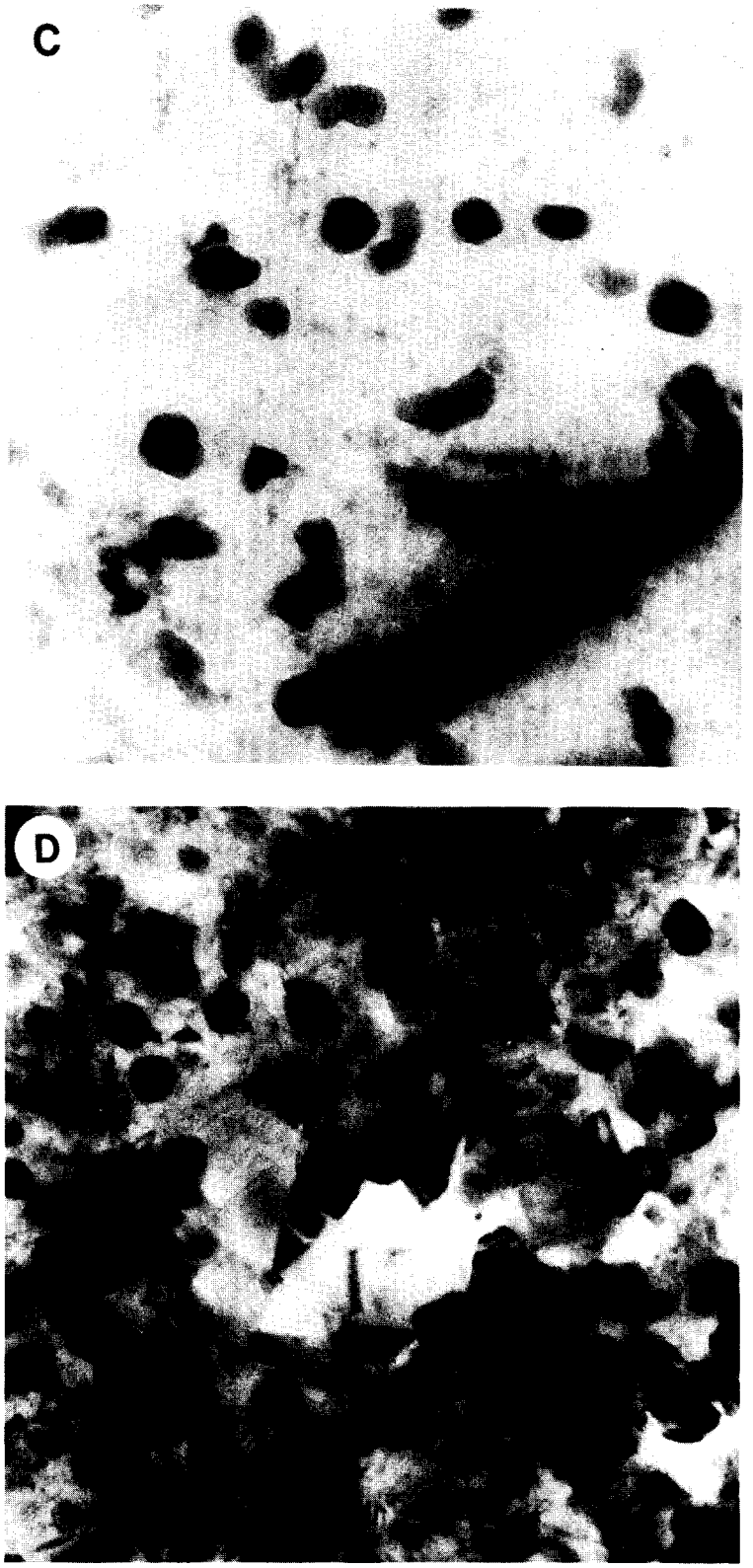


FIG. 2—*Continued.*

Finally, the nature of the coke formed on a reduced nickel/titanium oxide sample after reaction with a propylene/nitrogen (1 : 1 mixture) at 700°C for 0.5 h was investigated. Samples of the coke deposit were sprinkled onto transmission specimens of single crystal graphite used as a support. This combination was then heated in the presence of 2 Torr oxygen in the controlled atmosphere electron microscope and the oxidation characteristics of the coke determined (*17, 18*).

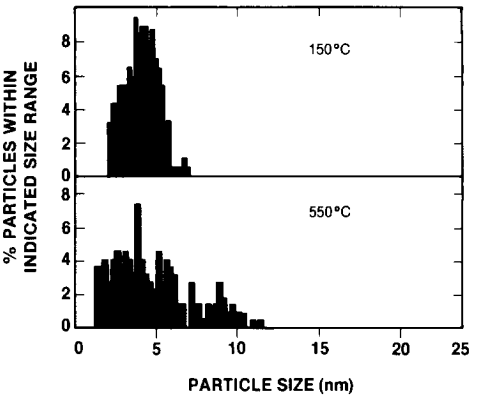


FIG. 3. Variation of PSD with reduction temperature for nickel on titanium oxide.

## RESULTS

### *Electron Microscopy Studies*

Figures 2A through D are transmission electron micrographs which show the change in appearance of nickel/titanium oxide specimens after reaction in hydrogen at temperatures up to 800°C. Figure 3 presents the corresponding particle size distributions at 150 and 550°C, respectively. Examination of these data indicates that although there is an increase in average particle size from 3.8 to 4.6 nm when reduction is performed at 550°C instead of 150°C, there is very little change in the particle morphology. The particles possess many of the characteristics exhibited by platinum on titanium oxide when treated under similar conditions (*9*). They have a faceted outline which in most cases tends to be hexagonal in form. The electron scattering density is uniform across a given particle, indicative of a flat rather than hemispherical profile. Although it is not possible to place a precise value on the thickness of the particles, there is little doubt that they are very thin relative to their lateral dimensions. Indeed, even though thin film specimens were used in this study and a special objective aperture was fitted in the microscope to improve the contrast, there was often difficulty in distinguishing nickel particles from the background of the oxide support. A few of the particles in Fig. 2A and B appear to be darker than the majority and may be thought to be thicker. However, this appearance is probably caused by a small deviation in the angle subtended by these particles with respect to the incident beam, compared with that presented by the majority of the particles. This creates diffraction contrast effects, an aspect which has been discussed in detail by Treacy and Howie (*19*).

A dramatic change in specimen appearance is observed after heating the system to 700°C (Fig. 2C). It is clear that there has been significant particle sintering and apparent loss of nickel from the surface. From this micrograph it is not possible to distinguish whether material has been removed from the support or has diffused into the oxide matrix. Many of the larger particles appear to be overlaying other particles and in this arrangement, one particle tends to retain the hexagonal outline, while the other has a more random diffuse form which can be described as "puddle-like."

There is a subtle change after the 800°C reduction treatment (Fig. 2D). Many more of the particles have assumed a faceted appearance, and there is less evidence of the "puddle-like" structures. It is also apparent that the particles have a higher electron scattering density than those shown in Figs. 2A and B, indicating that their morphology may no longer be that of a flat "pillbox" but could be more hemispherical. These observations suggest that the sintering process

has not only resulted in an increase in lateral dimensions but also in particle thickness. Because of the difficulty in accounting for all of the nickel at 700 and 800°C reduction temperatures, particle size distributions are not presented for these temperatures.

Selected area electron diffraction patterns have also been examined for each of these samples and provide information regarding change in the support structure. The pattern obtained from specimens treated at 150°C was diffuse rings and was identified as corresponding to the anatase structure of titanium dioxide. At the other extreme, at a reduction temperature of 800°C, a spot pattern was found and identified as being from a reduced form of titanium oxide, $Ti_4O_7$. At the intermediate treatment temperatures, 550 and 700°C, the pattern was complicated, consisting of contributions from both the above titanium oxide structures with the addition of the rutile form of the dioxide. These findings are completely consistent with those found earlier from reduction of the platinum/titanium oxide system (*9*). The failure to find any pattern corresponding to that of nickel is not unexpected in view of the dimensions of the particles.

TABLE 1

FMR Data on the Nickel–Titanium Oxide System

| Reduction temperature (°C) | Curie temperature (°C) | Relative degree of reduction (%) | |
|---|---|---|---|
| | | as[c] | as[d] |
| 300[a] | 316 | 98 | 89 |
| 400 | 316 | 95 | 95 |
| 550 | 316 | 57 | 59 |
| 700 | 333 | 100 | 100 |
| 860 | 343 | 95 | 84 |
| 550[b] | 348 | 49 | 49 |

[a] Sample was reduced for 3 h, all other reductions for 1 h.

[b] Sample previously reduced at 860°C and regenerated at 550°C by successive treatments in oxygen for 1.0 h and in hydrogen for 1.0 h.

[c] Values calculated from the $M^2$ versus $T$ (square of FMR intensity versus temperature) plots, as described in Ref. (*11*). The highest value of the degree of reduction was set equal to 100%.

[d] Values calculated by the double integration of the FMR spectra obtained at room temperature. The highest value of the reduction degree was set equal to 100%.

### *Ferromagnetic Resonance Studies*

Table 1 shows the measured values of the Curie temperatures and the apparent relative degree of reduction of a nickel on titanium oxide sample reduced at successively higher temperatures. After each reduction, the sample was quenched to room temperature and its thermomagnetic behavior studied. Following the final reduction at 860°C, the sample was "regenerated," i.e., heated in oxygen at 550°C for 1 h to break the SMSI effect (*1*) and subsequently reduced at the same temperature in hydrogen to regenerate it.

The variation in line-shape as a function of sample temperature during the FMR measurement is presented in Figs. 4A–C for each reduction temperature, where $H^+$, $H^0$, and $H^-$ correspond to the maximum, the crossing point, and the minimum values, respectively, of the first derivative of the FMR line as shown in Fig. 5.

The extent of hydrogen chemisorption was studied after reduction at 500 and 860°C. Neither the FMR intensity nor the line-shape or width values were found to change upon hydrogen desorption–adsorption. This confirms the lack of hydrogen chemisorption encountered previously on nickel–titanium oxide systems (*1, 2*). For example, Smith *et al.* (*4*) measured a coverage of hydrogen on nickel of 0.05 in the "SMSI" state. The FMR technique measures rapid chemisorption and, therefore, corresponds more closely to the data of Smith *et al.* (*4*) than that which will be discussed in a later section.

In a final series of reactions the regenerated sample and a sample which had been reduced at 250°C for 6 h were treated under

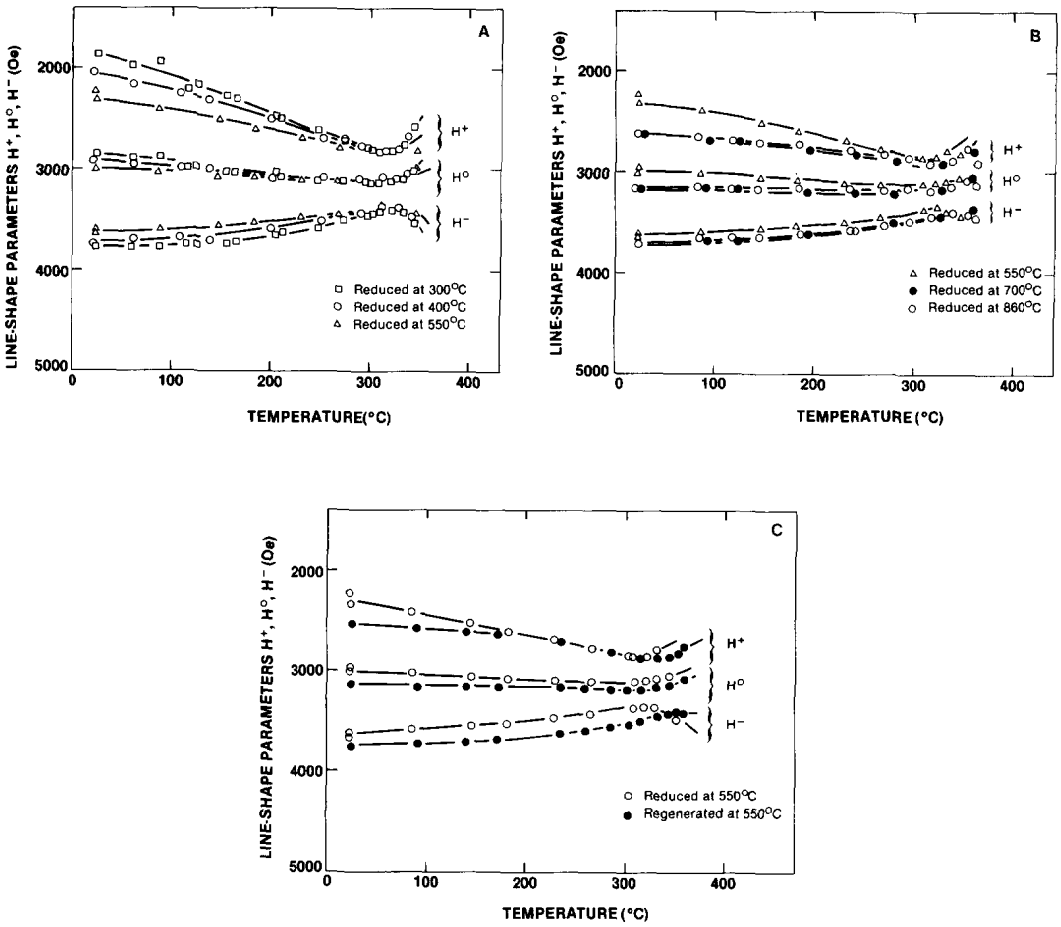


FIG. 4. FMR linewidths (Oe) as functions of measurement temperature following the treatments described in Table 1.

a propylene flow for 0.5 h at 700°C, and the form of carbon deposited during this reaction was characterized by selective oxidation in the controlled atmosphere electron microscope.

### *Characterization of Carbon Deposits by CAEM*

Carbon deposits usually have a complex structure consisting of several different growth forms, which can be divided into three main classes: amorphous, filamentous, and graphite platelets. In this study, attention was focused on the capacity of the system to produce filamentous carbon which requires the participation of metal catalyst particles (*17*). Earlier CAEM studies (*18*) have shown that when carbonaceous deposits are heated in 2–5 Torr oxygen, the amorphous component is removed first, followed by the filamentous form and finally the graphitic platelets undergo oxidation.

When the deposits produced from the interaction of nickel/titanium oxide samples with propylene were examined by this procedure, complete removal of the carbon was achieved on heating to 575°C in 2 Torr oxygen. No evidence for the existence of filamentous carbon was found in these samples.

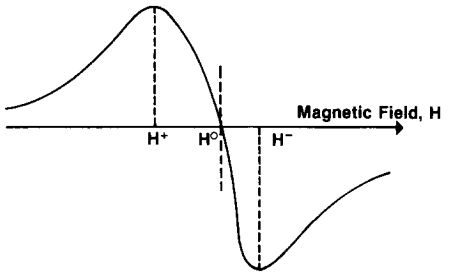


FIG. 5. The first derivative of the FMR line.

### *Surface Studies on a Geometrically Designed Model Catalyst*

The Auger spectra obtained after treatment of the model catalyst under various conditions are presented in Fig. 6. The initial surface of the sample exhibited only peaks attributable to nickel, oxygen, and a small amount of carbon contamination. This result is typical of an air-exposed nickel film. Upon reduction, however, a major restructuring of the surface was indicated. In those regions of the sample where the partially oxidized nickel film was in direct contact with the titanium oxide substrate, a strong titanium Auger signal was observed. In regions where the nickel film was separated from the titanium oxide by an interlayer of $SiO_2$, only nickel metal and a small residual carbon peak were detected. Critically, neither titanium nor silicon were detected in these latter regions.

Examination of this specimen in the scanning electron microscope showed it to have identical morphology to a similar untreated specimen. The surface showed no signs that particle nucleation or cracking of the nickel overlayer had taken place during the reduction treatment.

## DISCUSSION

In the past, the SMSI effect has been rationalized primarily in terms of an electronic charge transfer from the support to the metal (*20*). This metal–support interaction is then considered to be sufficiently strong to cause an electronic modification of the entire metal crystallite. In many of these studies, the metal has been very highly dispersed, and the electron transfer model has seemed reasonable. However, there are now several cases where the SMSI effect has been observed in systems containing relatively large particles (*5, 21, 22*), and these studies are beginning to cast doubts that the electron transfer model, as previously proposed (*20*), is the sole mechanism that accounts for SMSI. The present results, like those in references (*5, 21, 22*), require alternative explanations, along the lines discussed by Dumesic and co-workers (*22*). Caution, however, must be exercised in attempting to extend conclusions from large particle studies to include small particles and vice versa. Indeed, it has yet to be proven whether these two cases show SMSI properties of suppressed hydrogen and CO chemisorption for intrinsically similar reasons.

The micrographs presented in Fig. 2 provide interesting information about the nickel particle morphology in the present

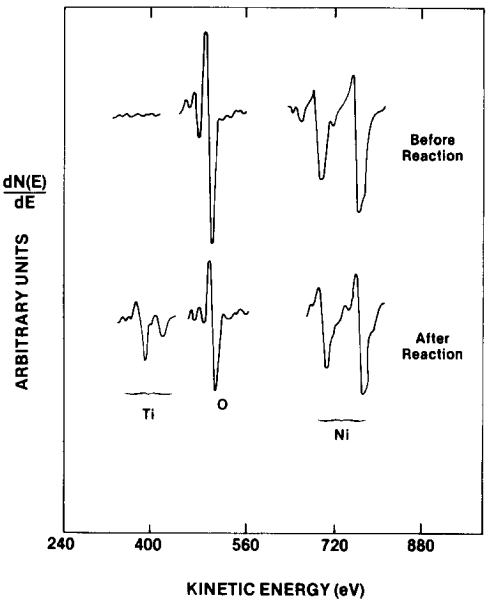


FIG. 6. Auger spectra of nickel/titanium oxide at start and after reaction in 1000 Torr hydrogen at 450°C for 45 min.

system. It should be appreciated that these are model systems presenting vast areas of relatively smooth support surface and in this regard may not be representative of a powdered catalyst surface. Even though José-Yacamán and co-workers (*23, 24*) have demonstrated that it is necessary to use sophisticated techniques in order to see *all* the small thin particles on a support, we believe that the micrographs obtained after the low-temperature reduction indicate that significant amounts of nickel are present as small thin particles with similar characteristics to platinum on titanium oxide (*9*). This is consistent with the observation of an additional low-temperature FMR line broadening typical of stress anisotropy when fresh powdered samples are reduced at low temperature.

After the 700°C reduction, the micrographs indicate the existence of two types of particle morphologies; pillbox and globular. Following the 800°C reduction, the micrographs show sintering and thickening of particles. Also Figs. 4A–C show that nickel particles reduced at the highest temperatures exhibit a line-shape variation with temperature that corresponds to a weak shape anisotropy. The near symmetry of these lines indicates that the nickel particles are almost spherical in the powdered catalyst. The sintering of nickel particles on titanium oxide is in sharp contrast to the behavior of the platinum/titanium oxide system where particle growth was inhibited (*9*). These observations lead to the conclusion that suppression of particle sintering is not necessarily a consequence of the establishment of the SMSI state.

Chemical information is also contained in the intensity and thermomagnetic parameters obtained from the FMR studies. After reduction at 300–400°C, the intensity of the FMR signal indicates that nickel is fully reduced. The Curie temperature derived from the thermomagnetic behavior of the sample is slightly lower than that of bulk nickel (316 versus 358°C), but this is typical of small supported crystallites. Similar results were found for nickel supported on silica, alumina, or zeolites (*25–29*). After the 550°C reduction, where the system should be in the SMSI state, the ferromagnetic intensity is only half of its previous value. There are two possibilities to account for this apparent 50% decrease in metallic character: (i) only 50% of the nickel is present as $Ni^0$, the remainder being nickel titanate, or (ii) 50% of the nickel is present as very thin crystallites (<3 monolayers thick) which, although they are fully reduced are not ferromagnetic due to their morphology. Though the present data do not allow us to differentiate between these two situations, the latter is favored based upon the TEM studies.

It is tempting to speculate that the 50% loss of ferromagnetism is due to the electronic SMSI effect. But, in the SMSI state, hydrogen chemisorption is suppressed by more than 50%. Furthermore, this is inconsistent with the results obtained at higher reduction temperatures where the magnetization is fully restored and the SMSI effect still persists. Indeed, after reduction at 860°C, the Curie temperature is very close to that of bulk nickel, as also found by other workers (*29*). Since the Curie temperature is very sensitive to electronic perturbations (*25*), previous mechanisms which invoke electronic interactions (*20*) can be discounted in the case of nickel on titanium oxide reduced at high temperature. Also, as stated previously, much lower Curie temperatures than the one measured here have been reported for nickel supported on other materials (*25–29*): cases where the hydrogen chemisorption properties were not affected.

The most reliable diagnostic of SMSI behavior is the suppression of hydrogen chemisorption (*3, 4*). FMR shows that this "definition" of SMSI has been satisfied by the samples reduced at elevated temperatures in the present study. However, recent work by Jiang *et al.* (*30*) demonstrates that even this definition of SMSI should be reconsidered. Nevertheless, after reduction

at 500 and 860°C (other reduction temperatures were not analyzed for this effect) and quenching to room temperature under hydrogen, neither the FMR intensity nor the line-shape or width values changed upon hydrogen desorption in flowing argon. Even when hydrogen desorption was effected at 400°C the room-temperature FMR line was unaffected. Previous studies of reduced nickel supported on silica or alumina showed pronounced effects of hydrogen chemisorption on both line shape and intensity (*15*).

In addition to changes in the nickel particle morphology (and perhaps chemical/electronic state), the titanium oxide support is transformed during the reduction process. The electron diffraction patterns demonstrate that as the reduction temperature is increased, the $TiO_2$ film changed from anatase to rutile and eventually to $Ti_4O_7$. It is possible that on prolonged reaction other reduced titanium oxides would have formed.

Auger analysis of the geometrically designed model catalyst indicates mobility of titanium–oxygen species in the system. Since this is a post-reaction examination, we must exercise caution in determining which particular species are mobile and from where they originate. We can neglect the possibility that titanium migrated onto the upper surface from the back of the foil during reduction in hydrogen at 450°C, since areas of the surface overlaying the silica disks were free of titanium. Furthermore, the presence of metallic titanium in the interior of the backing foil will have no effect (*31*). Large-scale fracturing of the nickel overlayer to reveal Auger detectable areas of underlying support does not seem probable because no Si signal is observed, a conclusion supported by SEM examination. However, it should be appreciated that the SEM will only resolve features greater than 6–10 nm in size. We believe that a sufficient yet small degree of fracturing occurred to allow migration of titanium–oxygen moieties onto the nickel. The difference in interfacial energies between the nickel and the support provides the driving force necessary for migration: reduced titanium oxide will have an appreciably higher tendency to migrate than silica (*32*).

To summarize, there appear to be at least two "forms" in which nickel exists (as evidenced by morphology and apparent degree of reduction), but both "forms" exhibit suppressed hydrogen chemisorption. The Curie temperature indicates that an electronic interaction alone cannot account for the present findings. Also, it is clear that following reduction a titanium–oxygen moiety exists on the nickel surface.

Choplin and co-workers (*30*) have suggested that the loss of hydrogen chemisorption capacity in reduced nickel/titanium oxide samples is related to the formation of NiTi alloys. This model seems to be unlikely as (a) it is difficult to reduce titanium oxide to the zero-valent state at 500°C, (b) the restoration of the original magnetization of nickel and the value of the Curie temperature above 550°C could hardly be explained by a phase segregation of the alloy or a reoxidation of the titanium, and (c) the formation of a NiTi alloy would dramatically affect the Curie temperature, which was not the case. Also, as discussed by Tauster and co-workers (*1, 2*) and recently by Meriaudeau and co-workers (*21*) intermetallic compounds containing titanium are generally made at very high temperatures usually above 1700°C. Furthermore, SMSI properties are drastically affected by exposure to air at 600°C, such a treatment should not be sufficient to affect a stable intermetallic compound.

The most plausible explanation which is consistent with the present results can be described in terms of a *decoration model.* In this model, a small amount of the oxide from around the metal particle periphery migrates onto the metal surface. The extent of the movement and decoration on the metal surface will depend on the gas environment, the temperature, and also the metal–oxide combination. Only a small

number of oxide moieties on the metal surface would be required to produce an interaction between the metal surface and this moiety. This interaction could be of the ligand-type, thus giving a chemical–electronic interaction between the moiety and the nickel *surface* atoms. Furthermore, the moiety could then influence changes in surface structure analogous to surface reconstruction in multicomponent systems or corrosive chemisorption with strongly adsorbing gases like NO (*34*). Due to the reducibility of the support, the oxide structure around the metal is severely affected. The interaction between metal atoms at the periphery of the particles and the surrounding "damaged" oxide structure would then constitute the first step toward movement of the oxide species onto the metal. The possibility of total encapsulation, i.e., that a complete oxide skin could form on the metal, may be possible for certain metal–oxide combinations at certain conditions (*6, 31*). However, at this stage the interaction should be such as to effectively block any reactions occurring at the catalyst surface (*6*). Indeed, the fact that reactions have been found to occur on similarly reduced $Ni/TiO_2$ catalysts (*5*) suggests that encapsulation has not taken place.

Another reaction in which supported nickel is an active catalyst is the formation of filamentous carbon during hydrocarbon decomposition (*17*) and so the finding of no filaments when reduced nickel/titanium oxide samples were reacted with acetylene is a very significant result. During filament growth, the metal catalyst particles are generally carried away from the support surface as a result of precipitation of dissolved carbon at the rear of the particle. In other systems where the particles are strongly held on the surface of the support, then the carbon is ejected from the particle by an extrusion mode (*17*). The failure to detect filaments in the present system indicates that the SMSI state involves more than a strong adherence of nickel to the support. Analogously, it was found that nickel carbonyl formation was suppressed for $Ni/TiO_2$ compared to $Ni/Al_2O_3$ (*5*) and $Ni/SiO_2$ (*35*).

Recent discussions (*6, 36*) in the literature pertaining to nickel/titanium oxide for CO hydrogenation have suggested that (a) the active sites are on the nickel surface (*36*), and (b) the active sites are only at the nickel–titanium oxide interface (*6*). Recently reported data (*30*) as well as those presented here indicate that nickel–titanium–oxygen interactions need not be limited to the particle support interface, but that formation of unique sites can take place on the particle itself. A similar decoration model has been proposed for iron on titanium oxide (*22*). The extent of coverage by the titanium–oxygen moieties, we believe, is a function of catalyst pretreatment, and the influence of this extent of coverage may be very different for different reactions. In the extreme, substantially increased reduction temperatures may result in encapsulation of the nickel with titanium–oxygen moieties, thus reducing CO hydrogenation activity and *n*-hexane hydrogenolysis as reported in Ref. (*6*).

The decoration model proposed here is also consistent with recent findings by Santos and Dumesic (*22*) who found that large iron particles supported on titanium oxide exhibited ammonia synthesis kinetic parameters and lack of CO chemisorption which were indicative of SMSI behavior, yet Mössbauer spectroscopy showed no evidence of an electronic effect in iron. Also, Haller and co-workers (*37, 38*) have observed that rhodium/titanium oxide in an SMSI state exhibited suppressed ethane hydrogenolysis activity and $H_2$ or CO chemisorption and thus behaved similarly to rhodium–silver clusters on silica. They also found that in the bimetallic system silver was predominantly on the surface of rhodium and acted as a blocking agent. According to these workers, the SMSI effect was strongest for small particles, and hence a particle size effect was associated with SMSI properties. They suggested that the

SMSI effect was a "poisoning" effect like silver on rhodium. Kugler and Garten (*7*) showed that bulk nickel could be induced to yield a product spectrum for $CO/H_2$ synthesis which mimicked that of nickel/titanium oxide if titanium–oxygen moieties were added to the bulk nickel surface.

The fact that oxides can cover metal particles and thus affect metal properties has been suggested previously. Schuit and van Reijen (*39*) claimed that "particle burying" was responsible for the loss of chemisorption capacity of nickel/silica catalysts following a reduction treatment. Recently Powell and Whittington (*40*) have presented electron microscopy evidence that platinum particles on silica became encapsulated when annealed at 1000°C and they suggested that partial encapsulation was possible at lower temperatures.

## CONCLUSIONS

A decoration model involving the formation of titanium–oxygen moieties on the surface of nickel crystallites which induces SMSI behavior has been proposed. The model is consistent with characterization studies of nickel/titanium oxide in terms of particle morphology, chemical state, and mobility of the components. Further experimental information will be required before this model can be claimed to be a general explanation for SMSI behavior.

## ACKNOWLEDGMENTS

The authors thank Dr. E. B. Prestridge for performing the high resolution electron microscopy examination, and Dr. L. L. Murrell, Dr. S. J. Tauster (both of CRSL, Exxon), and Professor J. A. Dumesic, University of Wisconsin, for valuable discussions.

## REFERENCES

1. Tauster, S. J., Fung, S. C., and Garten, R. L., *J. Amer. Chem. Soc.* **100,** 170 (1978).
2. Tauster, S. J., and Fung, S. C., *J. Catal.* **55,** 29 (1978).
3. Mustard, D. G., and Bartholomew, C. H., *J. Catal.* **67,** 186 (1981).
4. Smith, J. S., Thrower, P. A., and Vannice, M. A., *J. Catal.* **68,** 270 (1981).
5. Vannice, M. A., and Garten, R. L., *J. Catal.* **56,** 236 (1979).
6. Burch, R., and Flambard, A. R., *J. Catal.* **79,** 389 (1982).
7. Kugler, E. L., and Garten, R. L., U.S. Patent No. 4,273,724 (1981).
8. Kao, C. C., Tsai, S. C., Bahl, M. K., and Chung, Y. W., *Surf. Sci.* **95,** 1 (1980).
9. R. T. K. Baker, E. B. Prestridge, and R. L. Garten, *J. Catal.* **56,** 390 (1979).
10. Simoens, A. J., Derouane, E. G., and Baker, R. T. K., *J. Catal.* **73,** 175 (1982).
11. Selwood, P. W., "Chemisorption and Magnetization." Academic Press, New York, 1975.
12. Clausen, B. S., and Mørup, S., *Surf. Sci.* **82,** 1589 (1979).
13. Mørup, S., Clausen, B. S., and Topsøe, H., "International Conference on Mössbauer Spectroscopy, Portoroz, Yugoslavia, 1979."
14. Blum, J. K., and Göpel, W., *Thin Solid Films* **42,** 7 (1977).
15. Simoens, A. J., Ph.D. thesis, Univ. of Namur, Belgium, 1980.
16. Hardenbergh, J., and Dwyer, D. J., *J. Vac. Sci. Technol.*, in press.
17. Baker, R. T. K., and Harris, P. S., *in* "Chemistry and Physics of Carbon" (P. L. Walker, Jr., and P. A. Thrower, Eds.), Vol. 14, p. 83. Dekker, New York, 1978.
18. Baker, R. T. K., Alonzo, J. R., Dumesic, J. A., and Yates, D. J. C., *J. Catal.* **77,** 74 (1982).
19. Treacy, M. M. J., and Howie, A., *J. Catal.* **63,** 265 (1980).
20. Horsley, J. A., *J. Amer. Chem. Soc.* **101,** 2870 (1979).
21. Meriaudeau, P., Ellestad, O. H., Dufaux, M., and Naccache, C., *J. Catal.* **75,** 243 (1982).
22. Santos, J., Phillips, J., and Dumesic, J. A., *J. Catal.* **81,** 147 (1983).
23. José-Yacamán, M., and Dominguez, J. M., *J. Catal.* **67,** 475 (1981).
24. Gomez, A., Hernandez, P., and José-Yacamán, M., *Surf. Interface Anal.* **4,** 120 (1982).
25. Derouane, E. G., Simoens, A. J., Colin, C., Martin, G. A., Dalmon, J. A., and Vedrine, J. C., *J. Catal.* **52,** 50 (1978).
26. Simoens, A. J., and Derouane, E. G., *in* "Growth and Properties of Metal Clusters" (J. Bourdon, Ed.), pp. 201–207. Elsevier, Amsterdam, 1980.
27. Derouane, E. G., Simoens, A. J., and Vedrine, J. C., *Chem. Phys. Lett.* **52** 3, 549 (1977).
28. Jacobs, P. A., Mijs, H., Verdonk, J., Derouane, E. G., Gilson, J. P., and Simoens, A. J., *J. Chem. Soc. Faraday Trans. I* **75,** 1196 (1979).
29. Marcelin, G., and Lester, J. E., *Prepr. Div. Petrol. Chem. Amer. Chem. Soc.* **28,** 553 (1983).
30. Jiang, X-Z., Hayden, T. F., and Dumesic, J. A., *J. Catal.* **83,** 168 (1983).

*31.* Tatarchuk, B. J., and Dumesic, J. A., *J. Catal.* **70,** 335 (1981).
*32.* Overbury, S. H., Bertrand, P. A., and Somorjai, G. A., *Chem. Rev.* **75,** 547 (1975).
*33.* Choplin, A., Dalmon, J. A., and Martin, G. A., *C.R. Acad. Sci. Paris Ser. II* **293,** 37 (1981).
*34.* Yuen, S., Chen, Y., Kubsh, J. E., Dumesic, J. A., Topsøe, N., and Topsøe, H., *J. Phys. Chem.* **86,** 3022 (1982).
*35.* Dumesic, J. A., private communication.
*36.* Vannice, M. A., and Vasco-Jara, J., *in* "Metal-Support and Metal-Additive Effects in Catalysis" (B. Imelik, C. Naccache, G. Coudurier, H. Praliaud, P. Meriaudeau, P. Allezat, G. A. Martin, and J. C. Vedrine, Eds.), p. 185. Elsevier, New York, 1982.
*37.* Resasco, D. E., and Haller, G. L., "Studies in Surface Science and Catalysis," Vol. 11, p. 105. Elsevier, Amsterdam, 1982.
*38.* Resasco, D. E., and Haller, G. L., *Discuss. Faraday Soc.* **72,** 109 (1981).
*39.* Schuit, G. C. A., and van Reijen, L. L., "Advances in Catalysis," Vol. 10, p. 242. Academic Press, New York, 1958.
*40.* Powell, B. R., and Whittington, S. E., *J. Catal.* **81,** 382 (1983).